Hindawi
Advances in Materials Science and Engineering
Volume 2021, Article ID 6693326, 11 pages
https://doi.org/10.1155/2021/6693326

Research Article

Study of Nonlinear Deformation of FCC-AuCuSi under Pressure by the Statistical Moment Method

Nguyen Quang Hoc,[1] **Bui Duc Tinh**,[1] **Nguyen Duc Hien**,[2] **and Gelu Coman**[3]

[1]*Hanoi National University of Education, 136 Xuan Thuy, Hanoi, Vietnam*
[2]*Mac Dinh Chi High School, Chu Pah, Gia Lai, Vietnam*
[3]*"Dunarea de Jos" University of Galati, Galati, Romania*

Correspondence should be addressed to Bui Duc Tinh; tinhbd@hnue.edu.vn

Received 19 October 2020; Revised 8 February 2021; Accepted 17 February 2021; Published 5 March 2021

Academic Editor: Hamed Akhavan

In this work, we build the model and derive the theory of nonlinear deformation for substitutional alloy AB with interstitial atom C and face-centered cubic structure under pressure from the statistical moment method. The calculation results for FCC-AuCuSi are presented. We obtain the values of density of deformation energy, maximum real stress, limit of elastic deformation, and the stress-strain curve and compare the calculated results with experiments and other calculations.

1. Introduction

The study of elastic and thermodynamic properties of perfect ternary and binary interstitial alloys has also been attractive such as the theory of interstitial alloy [1], calculations from first principles, many-body potentials and dynamical dynamics for defects in metals, alloys and solid solutions [2–4] and elastic and thermodynamic properties of perfect ternary and binary interstitial alloys. We have studied the elastic deformation for body-entered cubic (BCC) and face-centered cubic (FCC) ternary and binary interstitial alloys under pressure by the statistical moment method (SMM) in [5–10].

The dependence of elastic and nonlinear deformations of materials on temperature, pressure, and concentration of components has very important role in predicting and understanding their interatomic interactions, strength, mechanical stability, phase transition mechanisms, and dynamical response. Silicides such as AuCuSi have attracted a lot of attention in recent years because of their functional applications and unusual physical properties. Gold silicide or gold silicon is one of the numerous metal alloys sold by American Elements under the trade name AE Alloys™.

The experimental data on the real stress and the limit of elastic deformation in the nonlinear deformation of pure metal Au are presented in [11–14].

Thermodynamic and mechanical properties of metals and interstitial alloys are studied by some theoretical methods and simulations. For example, Mehl and Papaconstantopoulos [15] applied a tight-binding (TB) scheme to extend first-principle calculations (*ab initio*) to regimes containing 10^2–10^3 atoms in a unit cell and used two-center, nonorthogonal tight-binding parameters and on-site terms. Numerical calculations for many metals are compared with *ab initio* calculations and experiments. Deformation mechanisms in the mechanical response of nanoporous gold are investigated by molecular dynamics simulations [16]. In addition, in recent years, some researchers have considered factors affecting the structure, the phase transformation, and the crystallization process of alloys AuCu [17], NiCu [18, 19], and AgCu [20].

In the present paper, we will study nonlinear deformation of FCC ternary alloy (substitutional alloy AB with interstitial atoms C) under pressure by the statistical moment method (SMM) [21–24]. In Section 2, we build the model and theoretical calculations, and in Section 3, we carry out numerical calculations for alloy AuCuSi.

2. Model and Theoretical Calculations

In our model, for interstitial alloy AC with FCC structure and concentration condition $c_C << c_A$ ($c_A = N_A/N$ is the

concentration of atoms A, N_A is the number of atoms A, $c_C = N_C/N$ is the concentration of atoms C, N_C is the number of atoms C, and $N = N_A + N_C$is the total number of atoms of the alloy AC), the cohesive energy u_0 and the alloy parameters $k, \gamma_1, \gamma_2, \gamma$ (k is called the harmonic parameter and $\gamma_1, \gamma_2, \gamma$ are called anharmonic parameters) for the interstitial atom C in face centers of cubic unit cell in the approximation of two coordination spheres have the form [5–10]

$$
\begin{aligned}
u_{0C} &= \frac{1}{2}\sum_{i=1}^{n_i}\varphi_{AC}(r_i) = 3\varphi_{AC}(r_{1C}) + 4\varphi_{AC}(r_{2C}),\\
r_{2C} &= \sqrt{3}r_{1C},\\
k_C &= \frac{1}{2}\sum_i\left(\frac{\partial^2\varphi_{AC}}{\partial u_{i\beta}^2}\right)_{\text{eq}} = \frac{\mathrm{d}^2\varphi_{AC}(r_{1C})}{\mathrm{d}r_{1C}^2} + \frac{2}{r_{1C}}\frac{\mathrm{d}\varphi_{AC}(r_{1C})}{\mathrm{d}r_{1C}} + \frac{4}{3}\frac{\mathrm{d}^2\varphi_{AC}(r_{2C})}{\mathrm{d}r_{2C}^2} + \frac{8}{3r_{2C}}\frac{\mathrm{d}\varphi_{AC}(r_{2C})}{\mathrm{d}r_{2C}},\\
\gamma_C &= 4(\gamma_{1C} + \gamma_{2C}),\\
\gamma_{1C} &= \frac{1}{48}\sum_i\left(\frac{\partial^4\varphi_{AC}}{\partial u_{i\beta}^4}\right)_{\text{eq}} = \frac{1}{24}\frac{\mathrm{d}^4\varphi_{AC}(r_{1C})}{\mathrm{d}r_{1C}^4} + \frac{1}{4r_{1C}^2}\frac{\mathrm{d}^2\varphi_{AC}(r_{1C})}{\mathrm{d}r_{1C}^2} - \frac{1}{4r_{1C}^3}\frac{\mathrm{d}\varphi_{AC}(r_{1C})}{\mathrm{d}r_{1C}} +\\
&\quad + \frac{1}{54}\frac{\mathrm{d}^4\varphi_{AC}(r_{2C})}{\mathrm{d}r_{2C}^4} + \frac{2}{9r_{2C}}\frac{\mathrm{d}^3\varphi_{AC}(r_{2C})}{\mathrm{d}r_{2C}^3} - \frac{2}{9r_{2C}^2}\frac{\mathrm{d}^2\varphi_{AC}(r_{2C})}{\mathrm{d}r_{2C}^2} + \frac{2}{9r_{2C}^3}\frac{\mathrm{d}\varphi_{AC}(r_{2C})}{\mathrm{d}r_{2C}},\\
\gamma_{2C} &= \frac{6}{48}\sum_i\left(\frac{\partial^4\varphi_{AC}}{\partial u_{i\alpha}^2\partial u_{i\beta}^2}\right)_{\text{eq}} = \frac{1}{2r_{1C}}\frac{\mathrm{d}^3\varphi_{AC}(r_{1C})}{\mathrm{d}r_{1C}^3} - \frac{3}{4r_{1C}^2}\frac{\mathrm{d}^2\varphi_{AC}(r_{1C})}{\mathrm{d}r_{1C}^2} + \frac{3}{4r_{1C}^3}\frac{\mathrm{d}\varphi_{AC}(r_{1C})}{\mathrm{d}r_{1C}} +\\
&\quad + \frac{1}{9}\frac{\mathrm{d}^4\varphi_{AC}(r_{2C})}{\mathrm{d}r_{2C}^4} + \frac{2}{3r_{2C}^2}\frac{\mathrm{d}^2\varphi_{AC}(r_{2C})}{\mathrm{d}r_{2C}^2} - \frac{2}{3r_{2C}^3}\frac{\mathrm{d}\varphi_{AC}(r_{2C})}{\mathrm{d}r_{2C}}.
\end{aligned}
\tag{1}
$$

The cohesive energy u_0 and the alloy parameters $k, \gamma_1, \gamma_2, \gamma$ for main metal atom A_1 in body center of cubic unit cell in the approximation of three coordination spheres have the form [5–10]

$$
\begin{aligned}
u_{0A_1} &= u_{0A} + \varphi_{AC}\left(r_{1A_1}\right),\\
k_{A_1} &= k_A + \frac{1}{2}\sum_i\left[\left(\frac{\partial^2\varphi_{AC}}{\partial u_{i\beta}^2}\right)_{\text{eq}}\right]_{r=r_{1A_1}} = k_A + \frac{\mathrm{d}^2\varphi_{AC}\left(r_{1A_1}\right)}{\mathrm{d}r_{1A_1}^2},\\
\gamma_{A_1} &= 4\left(\gamma_{1A_1} + \gamma_{2A_1}\right),\\
\gamma_{1A_1} &= \gamma_{1A} + \frac{1}{48}\sum_i\left[\left(\frac{\partial^4\varphi_{AC}}{\partial u_{i\beta}^4}\right)_{\text{eq}}\right]_{r=r_{1A_1}} = \gamma_{1A} + \frac{1}{24}\frac{\mathrm{d}^4\varphi_{AC}\left(r_{1A_1}\right)}{\mathrm{d}r_{1A_1}^4},\\
\gamma_{2A_1} &= \gamma_{2A} + \frac{6}{48}\sum_i\left[\left(\frac{\partial^4\varphi_{AC}}{\partial u_{i\alpha}^2\partial u_{i\beta}^2}\right)_{\text{eq}}\right]_{r=r_{1A_1}}\\
&= \gamma_{2A} + \frac{1}{4r_{1A_1}}\frac{\mathrm{d}^3\varphi_{AC}\left(r_{1A_1}\right)}{\mathrm{d}r_{1A_1}^3} - \frac{1}{2r_{1A_1}^2}\frac{\mathrm{d}^2\varphi_{AC}\left(r_{1A_1}\right)}{\mathrm{d}r_{1A_1}^2} + \frac{1}{2r_{1A_1}^3}\frac{\mathrm{d}\varphi_{AC}\left(r_{1A_1}\right)}{\mathrm{d}r_{1A_1}}.
\end{aligned}
\tag{2}
$$

The cohesive energy u_0 and the alloy parameters $k, \gamma_1, \gamma_2, \gamma$ for the main metal atom A_2 in corners of cubic unit cell in the approximation of three coordination spheres have the form [5–10]

$$
\begin{aligned}
u_{OA_2} &= u_{OA} + \varphi_{AC}\left(r_{1A_2}\right),\\
k_{A_2} &= k_A + \frac{1}{2}\sum_i \left[\left(\frac{\partial^2 \varphi_{AC}}{\partial u_{i\beta}^2}\right)_{\text{eq}}\right]_{r=r_{1A_2}} = k_A + \frac{1}{6}\frac{\mathrm{d}^2\varphi_{AC}\left(r_{1A_2}\right)}{\mathrm{d}r_{1A_2}^2} + \frac{23}{6r_{1A_2}}\frac{\mathrm{d}\varphi_{AC}\left(r_{1A_2}\right)}{\mathrm{d}r_{1A_2}},\\
\gamma_{A_2} &= 4\left(\gamma_{1A_2} + \gamma_{2A_2}\right),\\
\gamma_{1A_2} &= \gamma_{1A} + \frac{1}{48}\sum_i \left[\left(\frac{\partial^4 \varphi_{AC}}{\partial u_{i\beta}^4}\right)_{\text{eq}}\right]_{r=r_{1A_2}} = \gamma_{1A} + \frac{1}{54}\frac{\mathrm{d}^4\varphi_{AC}\left(r_{1A_2}\right)}{\mathrm{d}r_{1A_2}^4} + \frac{2}{9r_{1A_2}}\frac{\mathrm{d}^3\varphi_{AC}\left(r_{1A_2}\right)}{\mathrm{d}r_{1A_2}^3}\\
&\quad - \frac{2}{9r_{1A_2}^2}\frac{\mathrm{d}^2\varphi_{AC}\left(r_{1A_2}\right)}{\mathrm{d}r_{1A_2}^2} + \frac{2}{9r_{1A_2}^3}\frac{\mathrm{d}\varphi_{AC}\left(r_{1A_2}\right)}{\mathrm{d}r_{1A_2}},\\
\gamma_{2A_2} &= \gamma_{2A} + \frac{6}{48}\sum_i \left[\left(\frac{\partial^4 \varphi_{AC}}{\partial u_{i\alpha}^2 \partial u_{i\beta}^2}\right)_{\text{eq}}\right]_{r=r_{1A_2}} = \gamma_{2A} + \frac{1}{81}\frac{\mathrm{d}^4\varphi_{AC}\left(r_{1A_2}\right)}{\mathrm{d}r_{1A_2}^4}\\
&\quad + \frac{4}{27r_{1A_2}}\frac{\mathrm{d}^3\varphi_{AC}\left(r_{1A_2}\right)}{\mathrm{d}r_{1A_2}^3} + \frac{14}{27r_{1A_2}^2}\frac{\mathrm{d}^2\varphi_{AC}\left(r_{1A_2}\right)}{\mathrm{d}r_{1A_2}^2} - \frac{14}{27r_{1A_2}^3}\frac{\mathrm{d}\varphi_{AC}\left(r_{1A_2}\right)}{\mathrm{d}r_{1A_2}},
\end{aligned}
\tag{3}
$$

where ϕ_{AC} is the interaction potential between atoms A and C, $r_{1X} = r_{01X} + y_{0X}(T)$ is the nearest neighbor distance between the atom X ($X = A, A_1, A_2, C$) (A in clean metal and A_1, A_2, and C in interstitial alloy AC) and other atoms at temperature T, r_{01X} is the nearest neighbor distance between the atom X and other atoms at $T = 0$ K and is determined from the minimum condition of the cohesive energy u_{0X}, and $y_{0X}(T)$ is the displacement of atom X from equilibrium position at temperature T. $u_{0A}, k_A, \gamma_{1A}, \gamma_{2A}$ are the corresponding quantities in the clean metal A with FCC structure in the approximation of two coordination spheres and have the form [21, 22]

$$
\begin{aligned}
u_{0A} &= 6\varphi_{AA}(r_{1A}) + 3\varphi_{AA}(r_{2A}),\\
r_{2A} &= \sqrt{2}r_{1A},\\
k_A &= 2\frac{\mathrm{d}^2\varphi_{AA}(r_{1A})}{\mathrm{d}r_{1A}^2} + \frac{4}{r_{1A}}\frac{\mathrm{d}\varphi_{AA}(r_{1A})}{\mathrm{d}r_{1A}} + \frac{\mathrm{d}^2\varphi_{AA}(r_{2A})}{\mathrm{d}r_{2A}^2} + \frac{2}{r_{2A}}\frac{\mathrm{d}\varphi_{AA}(r_{2A})}{\mathrm{d}r_{2A}},\\
\gamma_{1A} &= \frac{1}{24}\frac{\mathrm{d}^4\varphi_{AA}(r_{1A})}{\mathrm{d}r_{1A}^4} + \frac{1}{4r_{1A}}\frac{\mathrm{d}^3\varphi_{AA}(r_{1A})}{\mathrm{d}r_{1A}^3} - \frac{1}{8r_{1A}^2}\frac{\mathrm{d}^2\varphi_{AA}(r_{1A})}{\mathrm{d}r_{1A}^2} + \frac{1}{8r_{1A}^3}\frac{\mathrm{d}\varphi_{AA}(r_{1A})}{\mathrm{d}r_{1A}}\\
&\quad + \frac{1}{24}\frac{\mathrm{d}^4\varphi_{AA}(r_{2A})}{\mathrm{d}r_{2A}^4} + \frac{1}{4r_{2A}^2}\frac{\mathrm{d}^2\varphi_{AA}(r_{2A})}{\mathrm{d}r_{2A}^2} - \frac{1}{4r_{2A}^3}\frac{\mathrm{d}\varphi_{AA}(r_{2A})}{\mathrm{d}r_{2A}},\\
\gamma_{2A} &= \frac{1}{48}\frac{\mathrm{d}^4\varphi_{AA}(r_{1A})}{\mathrm{d}r_{1A}^4} + \frac{7}{8r_{1A}}\frac{\mathrm{d}^3\varphi_{AA}(r_{1A})}{\mathrm{d}r_{1A}^3} - \frac{31}{16r_{1A}^2}\frac{\mathrm{d}^2\varphi_{AA}(r_{1A})}{\mathrm{d}r_{1A}^2} + \frac{31}{16r_{1A}^3}\frac{\mathrm{d}\varphi_{AA}(r_{1A})}{\mathrm{d}r_{1A}}\\
&\quad + \frac{1}{2r_{2A}}\frac{\mathrm{d}^3\varphi_{AA}(r_{2A})}{\mathrm{d}r_{2A}^3} - \frac{9}{8r_{2A}^2}\frac{\mathrm{d}^2\varphi_{AA}(r_{2A})}{\mathrm{d}r_{2A}^2} + \frac{9}{8r_{2A}^3}\frac{\mathrm{d}\varphi_{AA}(r_{2A})}{\mathrm{d}r_{2A}}.
\end{aligned}
\tag{4}
$$

The equations of state for FCC interstitial alloy at temperature T and pressure P and at 0 K and pressure P are written in the form [5, 6, 8–10, 23]

$$\begin{aligned} Pv &= -r_1\left[\frac{1}{6}\frac{\partial u_o}{\partial r_1} + \theta xcthx\frac{1}{2k}\frac{\partial k}{\partial r_1}\right], \\ v &= \frac{\sqrt{2}r_1^3}{2}, \\ Pv &= -r_1\left(\frac{1}{6}\frac{\partial u_0}{\partial r_1} + \frac{\hbar\omega_0}{4k}\frac{\partial k}{\partial r_1}\right). \end{aligned} \tag{5}$$

From that, we can calculate the nearest neighbor distance $r_{1X}(P,0)$ $(X = A, A_1, A_2, C)$, the parameters $k_X(P,0), \gamma_{1X}(P,0), \gamma_{2X}(P,0), \gamma_X(P,0)$, the displacement $y_{0X}(P,T)$ of atom X from equilibrium position as in [21], the nearest neighbor distance $r_{1X}(P,T)$, and the mean nearest neighbor distance between two atoms A in alloy $\overline{r_{1A}(P,T)}$ as follows [5, 6, 8–10]:

$$\begin{aligned} r_{1C}(P,T) &= r_{1C}(P,0) + y_{A_1}(P,T), \\ r_{1A}(P,T) &= r_{1A}(P,0) + y_A(P,T), \\ r_{1A_1}(P,T) &\approx r_{1B}(P,T), \\ r_{1A_2}(P,T) &= r_{1A_2}(P,0) + y_C(P,T), \\ \overline{r_{1A}(P,T)} &= \overline{r_{1A}(P,0)} + \overline{y(P,T)}, \\ \overline{r_{1A}(P,0)} &= (1-c_C)r_{1A}(P,0) + c_C r_{1A}'(P,0), r_{1A}'(P,0) = \sqrt{3}r_{1C}(P,0), \\ \overline{y(P,T)} &= (1-15c_C)y_A(P,T) + c_C y_C(P,T) + 6c_C y_{A_1}(P,T) + 8c_C y_{A_2}(P,T). \end{aligned} \tag{6}$$

The Helmholtz free energy of FCC interstitial alloy AC with the condition $c_C << c_A$ is determined by [5–10,21]

$$\begin{aligned} \psi_{AC} &= (1-15c_C)\psi_A + c_C\psi_C + 6c_C\psi_{A_1} + 8c_C\psi_{A_2} - TS_c, \\ \psi_X &\approx U_{0X} + \psi_{0X} + 3N\left\{\frac{\theta^2}{k_X^2}\left[\gamma_{2X}Y_X^2 - \frac{2\gamma_{1X}}{3}\left(1+\frac{Y_X}{2}\right)\right]\right. \\ &\quad + \frac{2\theta^3}{k_X^4}\left\{\left[\frac{4}{3}\gamma_{2X}Y_X\left(1+\frac{Y_X}{2}\right) - 2\left[\gamma_{1X}^2 + 2\gamma_{1X}\gamma_{2X}\right]\right.\right. \\ &\quad \left.\left.\left(1+\frac{Y_X}{2}\right)(1+Y_X)\right], \\ \psi_{0X} &= 3N\theta\left[x_X + \ln\left(1-e^{-2x_X}\right)\right], \\ Y_X &\equiv x_X \coth x_X, \end{aligned} \tag{7}$$

where ψ_X is the Helmholtz free energy of one atom X, U_{0X} is the cohesive energy, and S_c is the configurational entropy of FCC interstitial alloy AC.

The nearest neighbor distances between two atoms in alloy AC after deformation have the form [9]

$$\begin{aligned} r_{01X}^F &= r_{01X}(1+\varepsilon), \\ r_{1X}^F(P,0) &= r_{1X}(P,0)\left(1+2\varepsilon+\varepsilon^2\right) \\ r_{1C}^F(P,T) &= r_{01C}^F(P,0) + y_{A_1}^F(P,0), \\ r_{1A}^F(P,0) &= r_{01A}^F(P,0) + y_A^F(P,T), \\ r_{1A_1}^F(P,T) &\approx r_{1C}^F(P,T), \\ r_{1A_2}^F(P,T) &= r_{01A_2}^F(P,0) + y_C^F(P,T). \end{aligned} \tag{8}$$

The mean nearest neighbor distances between two atoms A in interstitial alloy AC at pressure P and temperature T after deformation have the form [9]

$$\begin{aligned} \overline{r_{1A}^{ACF}(P,T)} &= \overline{r_{01A}^{ACF}(P,0)} + \overline{y^{ACF}(P,T)}, \\ \overline{r_{01A}^{ACF}(P,0)} &= \left[(1-c_C)r_{01A}^F(P,0) + c_C r_{01A}^{'ACF}(P,0)\right]\left(1+2\varepsilon+\varepsilon^2\right), \\ r_{01A}^{'F}(P,0) &= \sqrt{3}r_{01C}^F(P,0), \\ \overline{y^{ACF}(P,T)} &= (1-15c_C)y_A^F(P,T) + c_C y_C^F(P,T) + 6c_C y_{A_1}^F(P,T) + 8c_C y_{A_2}^F(P,T). \end{aligned} \tag{9}$$

The mean nearest neighbor distances between two atoms A in substitutional alloy AB with interstitial atoms C at pressure P and temperature T and at pressure P and temperature $T = 0\,\mathrm{K}$ after deformation have the form [5, 6, 9]

$$
\begin{aligned}
a^F_{ABC} &= c_{AC}a^F_{AC}\frac{B^F_{TAC}}{\overline{B^{\mathrm{bcc}F}_T}} + c_B a^F_B \frac{B^F_{TB}}{\overline{B^F_T}},\\
\overline{B^F_T} &= c_{AC}B^F_{TAC} + c_B B^F_{TB},\\
c_{AC} &= c_A + c_C,\\
a^F_{ABC} &\equiv \overline{r^{ABCF}_{1A}(P,T)},\\
a^F_{AC} &\equiv \overline{r^{ACF}_{1A}(P,T)},\\
a^F_B &\equiv r^F_{1B}(P,T),\\
B^F_{TAC} &= \frac{1}{\chi^F_{TAC}}\\
B^F_{TB} &= \frac{1}{\chi^F_{TB}}\\
\left(\frac{\partial^2\psi^F_{AC}}{\partial a^{F2}_{AC}}\right)_T &\approx (1-15c_C)\left(\frac{\partial^2\psi^F_A}{\partial a^{F2}_A}\right)_T + c_C\left(\frac{\partial^2\psi^F_C}{\partial a^{F2}_C}\right)_T + 6c_C\left(\frac{\partial^2\psi^F_{A_1}}{\partial a^{F2}_{A_1}}\right)_T + 8c_C\left(\frac{\partial^2\psi^F_{A_2}}{\partial a^{F2}_{A_2}}\right)_T,\\
\frac{1}{3N}\left(\frac{\partial^2\psi^F_X}{\partial a^{F2}_X}\right)_T &= \frac{1}{6}\frac{\partial^2 u^F_{0X}}{\partial a^{F2}_X} + \frac{\hbar\omega^F_X}{4k^F_X}\left[\frac{\partial^2 k^F_X}{\partial a^{F2}_X} - \frac{1}{2k^F_X}\left(\frac{\partial k^F_X}{\partial a^F_X}\right)^2\right],\\
X &= A, A_1, A_2, B, C,\\
a^F_{0ABC} &= c_{AC}a^F_{0AC}\frac{B^F_{0TAC}}{\overline{B^F_{0T}}} + c_B a^F_{0B}\frac{B^F_{0TB}}{\overline{B^F_{0T}}},\\
\overline{B^F_{0T}} &= c_{AC}B^F_{0TAC} + c_B B^F_{0TB},\\
a^F_{0ABC} &\equiv \overline{r^{ABCF}_{01A}(P,0)},\\
a^F_{0AC} &\equiv \overline{r^{ACF}_{01A}(P,0)},\\
a^F_{0B} &\equiv r^F_{01B}(P,0).
\end{aligned}
\tag{10}
$$

The Helmholtz free energy of alloy ABC before and after deformation with the condition $c_C << c_B << c_A$ is determined by [5, 6, 9]

$$
\begin{aligned}
\psi_{ABC} &= \psi_{AC} + c_B(\psi_B - \psi_A) + TS^{AC}_c - TS^{ABC}_c,\\
\psi_{AC} &= (1-15c_C)\psi_A + c_C\psi_C + 6c_C\psi_{A_1} + 8c_C\psi_{A_2} - TS^{AC}_c,\\
\psi^F_{ABC} &= \psi^F_{AC} + c_B\left(\psi^F_B - \psi^F_A\right) + TS^{ACF}_c - TS^{ABCF}_c,\\
\psi^F_{AC} &= (1-15c_C)\psi^F_A + c_C\psi^F_C + 6c_C\psi^F_{A_1} + 8c_C\psi^F_{A_2} - TS^{ACF}_c.
\end{aligned}
\tag{11}
$$

The relationship between the stress and the deformation in nonlinear deformation is given by [9]

$$
\sigma_{1ABC} = \sigma_{0ABC}\frac{\varepsilon^{\alpha_{ABC}}}{1+\varepsilon},
\tag{12}
$$

where $\sigma_{0\mathrm{ABC}}$ and α_{ABC} are constants for every alloy.

The density of deformation energy can be written in the form [9]

$$
\begin{aligned}
f_{ABC}(\varepsilon) = {} & \frac{1}{N}(1-c_A)\left\{\psi_A\left(\frac{1}{\nu^F_{ABC}}-\frac{1}{\nu_{ABC}}\right)+\frac{2\varepsilon r^F_{01A}}{\nu^F_{ABC}}\left(\frac{\partial\psi^F_A}{\partial r^F_{1A}}\right)_T+\frac{\varepsilon^2}{2\nu^F_{ABC}}\left[\left(\frac{\partial^2\psi^F_A}{\partial r^{F2}_{1A}}\right)_T\left(2r^F_{01A}\right)^2+\left(\frac{\partial\psi^F_A}{\partial r^F_{1A}}\right)_T 2r^F_{01A}\right]\right\}+\\
& +\frac{c_C}{N}\left\{\psi_B\left(\frac{1}{\nu^F_{ABC}}-\frac{1}{\nu_{ABC}}\right)+\frac{2\varepsilon r^F_{01B}}{\nu^F_{ABC}}\left(\frac{\partial\psi^F_B}{\partial r^F_{1B}}\right)_T+\frac{\varepsilon^2}{2\nu^F_{ABC}}\left[\left(\frac{\partial^2\psi^F_B}{\partial r^{F2}_{1B}}\right)_T\left(2r^F_{01B}\right)^2+\left(\frac{\partial\psi^F_B}{\partial r^F_{1B}}\right)_T 2r^F_{01B}\right]\right\}+\\
& +\frac{c_{A_1}}{N}\left\{\psi_{A_1}\left(\frac{1}{\nu^F_{ABC}}-\frac{1}{\nu_{ABC}}\right)+\frac{2\varepsilon r^F_{01A_1}}{\nu^F_{ABC}}\left(\frac{\partial\psi^F_{A_1}}{\partial r^F_{1A_1}}\right)_T+\frac{\varepsilon^2}{2\nu^F_{ABC}}\left[\left(\frac{\partial^2\psi^F_{A_1}}{\partial r^{F2}_{1A_1}}\right)_T\left(2r^F_{01A_1}\right)^2+\left(\frac{\partial\psi^F_{A_1}}{\partial r^F_{1A_1}}\right)_T 2r^F_{01A_1}\right]\right\}+\\
& +\frac{c_{A_2}}{N}\left\{\psi_{A_2}\left(\frac{1}{\nu^F_{ABC}}-\frac{1}{\nu_{ABC}}\right)+\frac{2\varepsilon r^F_{01A_2}}{\nu^F_{ABC}}\left(\frac{\partial\psi^F_{A_2}}{\partial r^F_{1A_2}}\right)_T+\frac{\varepsilon^2}{2\nu^F_{ABC}}\left[\left(\frac{\partial^2\psi^F_{A_2}}{\partial r^{F2}_{1A_2}}\right)_T\left(2r^F_{01A_2}\right)^2+\left(\frac{\partial\psi^F_{A_2}}{\partial r^F_{1A_2}}\right)_T 2r^F_{01A_2}\right]\right\}+\\
& +\frac{c_B}{N}\left\{\psi_B\left(\frac{1}{\nu^F_{ABC}}-\frac{1}{\nu_{ABC}}\right)+\frac{2\varepsilon r^F_{01B}}{\nu^F_{ABC}}\left(\frac{\partial\psi^F_B}{\partial r^F_{1B}}\right)_T+\frac{\varepsilon^2}{2\nu^F_{ABC}}\left[\left(\frac{\partial^2\psi^F_B}{\partial r^{F2}_{1B}}\right)_T\left(2r^F_{01B}\right)^2+\left(\frac{\partial\psi^F_B}{\partial r^F_{1B}}\right)_T 2r^F_{01B}\right]\right\}-\\
& -\frac{c_B}{N}\left\{\psi_A\left(\frac{1}{\nu^F_{ABC}}-\frac{1}{\nu_{ABC}}\right)+\frac{2\varepsilon r^F_{01A}}{\nu^F_{ABC}}\left(\frac{\partial\psi^F_A}{\partial r^F_{1A}}\right)_T+\frac{\varepsilon^2}{2\nu^F_{ABC}}\left[\left(\frac{\partial^2\psi^F_A}{\partial r^{F2}_{1A}}\right)_T\left(2r^F_{01A}\right)^2+\left(\frac{\partial\psi^F_A}{\partial r^F_{1A}}\right)_T 2r^F_{01A}\right]\right\}.
\end{aligned}
\tag{13}
$$

When the deformation rate is constant, the density of deformation energy of alloy is determined by [9]

$$
f_{ABC}(\varepsilon) = C_{ABC}\cdot\sigma_{ABC}\cdot\varepsilon, \tag{14}
$$

where C_{ABC} is the proportional factor. At the maximum value of the density of deformation energy, we have

$$
f_{ABC}\left(\varepsilon^F_{ABC}\right) = f_{ABC\max} = C_{ABC}\sigma_{ABC\max}\varepsilon^F_{ABC}. \tag{15}
$$

The maximum value of stress $\sigma_{ABC\max}$ and the maximum real stress $\sigma_{1ABC\max}$ are [9]

$$
\begin{aligned}
\sigma_{ABC\max} &= \frac{f_{ABC\max}}{C_{ABC}\varepsilon^F_{ABC}},\\
\sigma_{1ABC\max} &= \frac{\sigma_{ABC\max}}{1+\varepsilon^F_{ABC}} = \frac{f_{ABC\max}}{C_{ABC}\varepsilon^F_{ABC}\left(1+\varepsilon^F_{ABC}\right)}.
\end{aligned}
\tag{16}
$$

From the maximum condition of stress $(\partial\sigma_{1ABC}/\partial\varepsilon)_{\varepsilon^F_{ABC}} = 0$, we derive the deformation ε^F_{ABC} corresponding to the maximum value of real stress as follows [9]:

$$
\varepsilon^F_{ABC} = \frac{\alpha_{ABC}}{1-\alpha_{ABC}} \Rightarrow \sigma_{1ABC\max} = \sigma_{0ABC}\frac{\left(\varepsilon^F_{ABC}\right)^{\alpha_{ABC}}}{1+\varepsilon^F_{ABC}}. \tag{17}
$$

C_{ABC} is determined from the experimental condition of stress $\sigma_{0,2ABC}$ in alloy in the form [9]

$$
C_{ABC} = \frac{f_{ABC}\left(\varepsilon_{0.2}\right)}{\sigma_{0.2ABC}\varepsilon_{0.2}}. \tag{18}
$$

From the obtained value of ε^F_{ABC}, we can calculate σ_{0ABC} and α_{ABC}. The limit of elastic deformation $\sigma_e = E_{ABC}\varepsilon_e$ of alloy ABC is determined by [9]

$$
\sigma_e = E_{ABC}\varepsilon_e = \sigma_{0ABC}\frac{\varepsilon^\alpha_e}{1+\varepsilon_e}. \tag{19}
$$

Here E_{ABC} is Young's modulus of alloy ABC and has the form [5, 6]

$$
\begin{aligned}
E_{ABC} &= c_B\left(E_B-E_A\right)+E_{AC},\\
E_Y &= \frac{1}{\pi\cdot r_{1Y}\cdot A_{1Y}},\\
A_{1Y} &= \frac{1}{k_Y}\left[1+\frac{2\gamma^2_Y\theta^2}{k^4_Y}\left(1+\frac{1}{2}x_Y cthx_Y\right)\left(1+x_Y cthx_Y\right)\right], \quad x_Y = \frac{\hbar\omega_Y}{2\theta}, Y = A, B,\\
E_{AC} &= E_A\left(1-15c_C+c_C\frac{\left(\partial^2\psi_C/\partial\varepsilon^2\right)+6\left(\partial^2\psi_{A_1}/\partial\varepsilon^2\right)+8\left(\partial^2\psi_{A_2}/\partial\varepsilon^2\right)}{\left(\partial^2\psi_A/\partial\varepsilon^2\right)}\right),\\
\frac{\partial^2\psi_X}{\partial\varepsilon^2} &= \left\{\frac{1}{2}\frac{\partial^2U_{0X}}{\partial r^2_{1X}}+\frac{3}{4}\frac{\hbar\omega_X}{k_X}\left[\frac{\partial^2k_X}{\partial r^2_{1X}}-\frac{1}{2k_X}\left(\frac{\partial k_X}{\partial r_{1X}}\right)\right]^2\right\}4r^2_{01X}+\\
&\quad +\left(\frac{1}{2}\frac{\partial U_{0X}}{\partial r_{1X}}+x_X cthx_X\frac{3\theta}{2k_X}\frac{\partial k_X}{\partial r_{1X}}\right)2r_{01X}, \quad x_X = \frac{\hbar\omega_X}{2\theta}, \omega_X = \sqrt{\frac{k_X}{m_X}}, X = A, A_1, A_2, C.
\end{aligned}
\tag{20}
$$

Table 1: Mie–Lennard-Jones potential parameters for interactions Au-Au, Cu-Cu, and Si-Si.

Interaction	D/k_B (K)	r_0 (10^{-10} m)	m	n
Au-Au [27]	7411.5	2.8751	1.96	15.56
Cu-Cu [27]	6841.3	2.5487	3.03	8.37
Si-Si [25]	32701.7	2.295	6	12

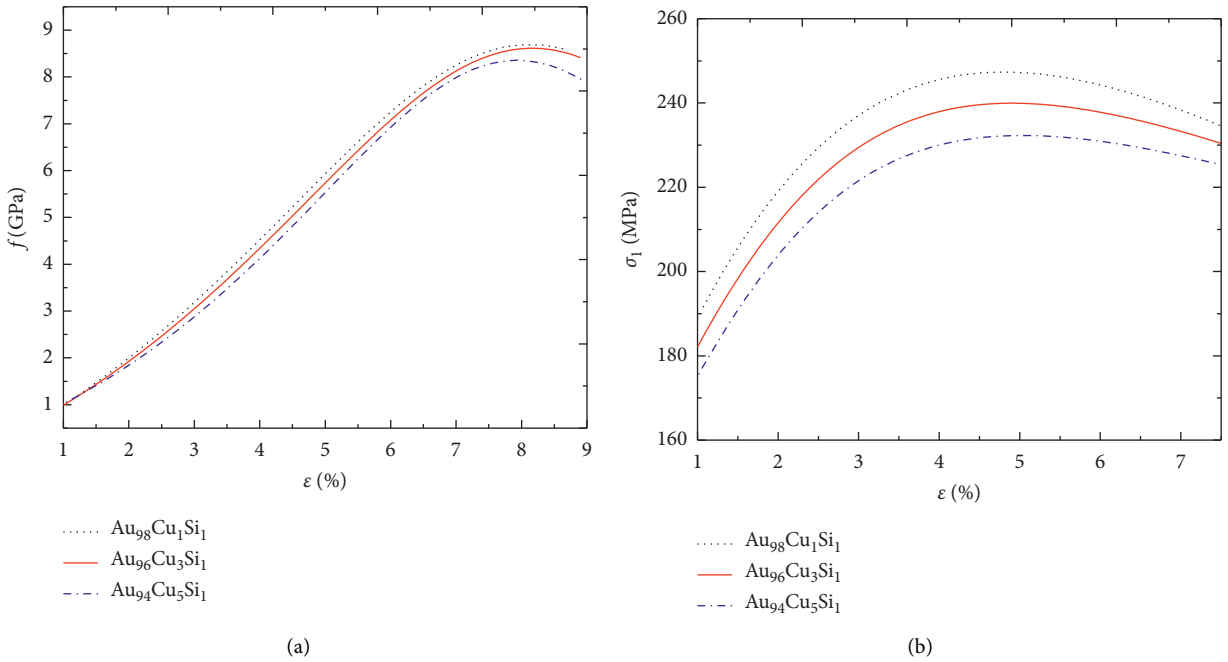

(a) (b)

Figure 1: The density of deformation energy $f(\varepsilon)$ (a) and the real stress $\sigma_1(\varepsilon)$ (b) of $Au_{99-x}Cu_xSi_1$ at $T = 300$ K and $P = 0$ calculated by the SMM.

Here E_{AC}, E_A, E_B are Young's moduli of alloy AC and metals A, B, respectively.

3. Numerical Results for Alloy AuCuSi

To describe the interaction between atoms Au and Si, we apply the Mie–Lennard-Jones pair interaction potential in the form [25]

$$\varphi(r) = \frac{D}{n-m}\left[m\left(\frac{r_0}{r}\right)^n - n\left(\frac{r_0}{r}\right)^m\right], \tag{21}$$

where D is the depth of potential well corresponding to the equilibrium distance r_0 and m and n are determined empirically. Then, the potential parameters for the interaction Au-Si are determined by [26]

$$D_{\text{Au–Si}} = \sqrt{D_{\text{Au–Au}} D_{\text{Si–Si}}},$$
$$r_{0\text{Au–Si}} = \frac{1}{2}\left(r_{0\text{Au–Au}} + r_{0\text{Si–Si}}\right). \tag{22}$$

We find $m_{\text{Au-Si}}$ and $n_{\text{Au-Si}}$ by fitting the theoretical result with the experimental data for Young's modulus of interstitial alloy $AuSi_{3\%}$ at room temperature. The Mie–Lennard-Jones potential parameters for the interactions Au-Au, Si-Si, and Au-Si are given in Table 1. The Poisson ratio is 0.42 for Au [28], 0.34 for Cu [29], and 0.21 for Si [30]. Our investigated range of temperature up to 900 K is below the melting temperature of Au, Cu, and Si in the range of pressure from zero to 6 GPa as studies on the melting curve for these materials [31–33].

From

$$E = \frac{\sigma_{0,2}}{\varepsilon_{0,2}} \Longrightarrow \sigma_{0,2} = E\varepsilon_{0,2} = E \times 0.2\%, \tag{23}$$

the experimental value of Young's modulus $E = 89.1.10^9$ Pa for Au at $T = 300$ K and $P = 0$ [34]. From that, we obtain $\sigma_{0.2} = 89.1 \times 10^9 \times 0.002 = 178.2 \times 10^6$ Pa. Figure 1 shows the density of deformation energy $f(\varepsilon)$ and the real stress $\sigma_1(\varepsilon)$of AuCuSi at $T = 300$ K, $P = 0$, $c_{\text{Si}} = 1\%$, and $c_{\text{Cu}} = 1$, 3, and 5% calculated by the SMM. For AuCuSi at the same temperature, pressure, and concentration of interstitial atoms, when the concentration of substitutional atoms increases, the maximum real stress decreases by 2% and the elastic limit also decreases by 2%. The density of deformation energy has the maximum value when the strain $\varepsilon_F = 0.08$, and from that, we can find the maximum real stress $\sigma_{1\,\max}$,the elastic limit σ_e, and the elastic strain ε_e for AuCuSi as shown in Table 2.

Table 2: Values of ε_F ($f(\varepsilon_F) = f_{\max}$), $\sigma_{1\max}$, σ_e, and ε_e of $Au_{99-x}Cu_xSi_1$ at $P = 0$ and $T = 300$ K calculated by the SMM.

	ε_F (%)	$\sigma_{1\max}$ (MPa)	ε_e (%)	σ_e (MPa)
$Au_{98}Cu_1Si_1$	8.0	231.79	0.21	190.84
$Au_{96}Cu_3Si_1$	8.0	230.38	0.21	189.40
$Au_{94}Cu_5Si_1$	8.0	227.06	0.20	186.38

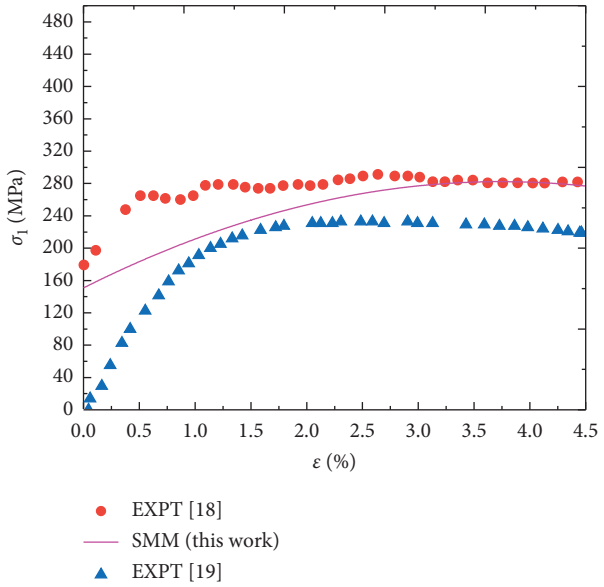

Figure 2: The real stress $\sigma_1(\varepsilon)$ of Au at $T = 300$ K and $P = 0$ calculated by the SMM and from EXPT [11] and EXPT [12].

When concentrations $c_{Cu}, c_{Si} \longrightarrow 0$, we obtain the nonlinear deformation of main metal Au. Figure 2 shows the curve of real stress $\sigma_1(\varepsilon)$ for Au at $P = 0$ and $T = 300$ K where we have the comparison between the SMM and experiments [11, 12]. The maximum real stress $\sigma_{1\max}$ and the elastic limit σ_e calculated by the SMM in Table 3 are in good agreement with the molecular dynamics (MD) results [16] and experiments [13, 14]. The error of the maximum real stress between the SMM calculation and the MD result [16] is 0.6%. The error of the elastic limit between the SMM calculation and the experimental data [13] is 5.65%. Thus, the SMM calculations of the maximum real stress and the elastic limit for Au at $P = 0$ and $T = 300$ K are in good agreement with other calculations and experiments.

Figure 3 shows the density of deformation energy $f(\varepsilon)$ and the real stress $\sigma_1(\varepsilon)$ of AuCuSi at $T = 300$ K, $P = 0$, $c_{Cu} = 10\%$, and $c_{Si} = 0$, 1, and 2% calculated by the SMM. For AuCuSi at the same temperature, pressure, and concentration of substitutional atoms, when the concentration of interstitial atoms increases, the maximum real stress and the elastic limit decrease strongly. We have the comparison on values of ε_F, σ_{1max}, ε_e, and σ_e for alloys AuSi, AuCu, and AuCuSi in Table 4.

Figure 4 shows the density of deformation energy $f(\varepsilon)$ and the real stress $\sigma_1(\varepsilon)$ of AuCuSi at $T = 300$, 600, and 900 K, $P = 0$, $c_{Cu} = 10\%$, and $c_{Si} = 2\%$ calculated by the SMM. For AuCuSi at the same pressure, concentration of substitutional atoms, and concentration of interstitial atoms, when the temperature increases, the maximum real stress and the elastic limit increase. We have the comparison on values of ε_F, σ_{1max}, ε_e, and σ_e for $Au_{88}Cu_{10}Si_2$ at $P = 0$ and $T = 300$, 600, and 900 K in Table 5.

Table 3: Values of ε_F ($f(\varepsilon_F) = f_{\max}$), $\sigma_{1\max}$, ε_e, and σ_e for Au at $P = 0$ and $T = 300$ K calculated by the SMM and from MD [16], EXPT [13], and EXPT [14].

$\sigma_{1\max}$ (MPa)			σ_e (MPa)			
SMM		MD [16]	SMM		EXPT [13]	EXPT [14]
$\varepsilon_F = 9.6\%$	243.52	245	$\varepsilon_e = 0.19\%$	188.70	200	45 ÷ 300

Figure 5 shows the real stress $\sigma_1(\varepsilon)$ of AuCuSi at $T = 300$ K, $P = 2$, 4, and 6 GPa, $c_{Cu} = 10\%$, and $c_{Si} = 3\%$ calculated by the SMM. For AuCuSi at the same temperature, concentration of substitutional atoms, and concentration of interstitial atoms, when the pressure increases, the maximum real stress increases and the elastic limit decreases. When the pressure increases from 2 to 4 GPa, the maximum real stress increases by 3% and the elastic limit decreases by 7.86%. When the pressure increases from 4 to 6 GPa, the maximum real stress increases by 11% and the elastic limit decreases by 10.56%. We have the comparison on values of ε_F, $\sigma_{1\max}$, ε_e, and σ_e for $Au_{87}Cu_{10}Si_3$ at $P = 2$, 4, and 6 GPa and $T = 300$ K in Table 6.

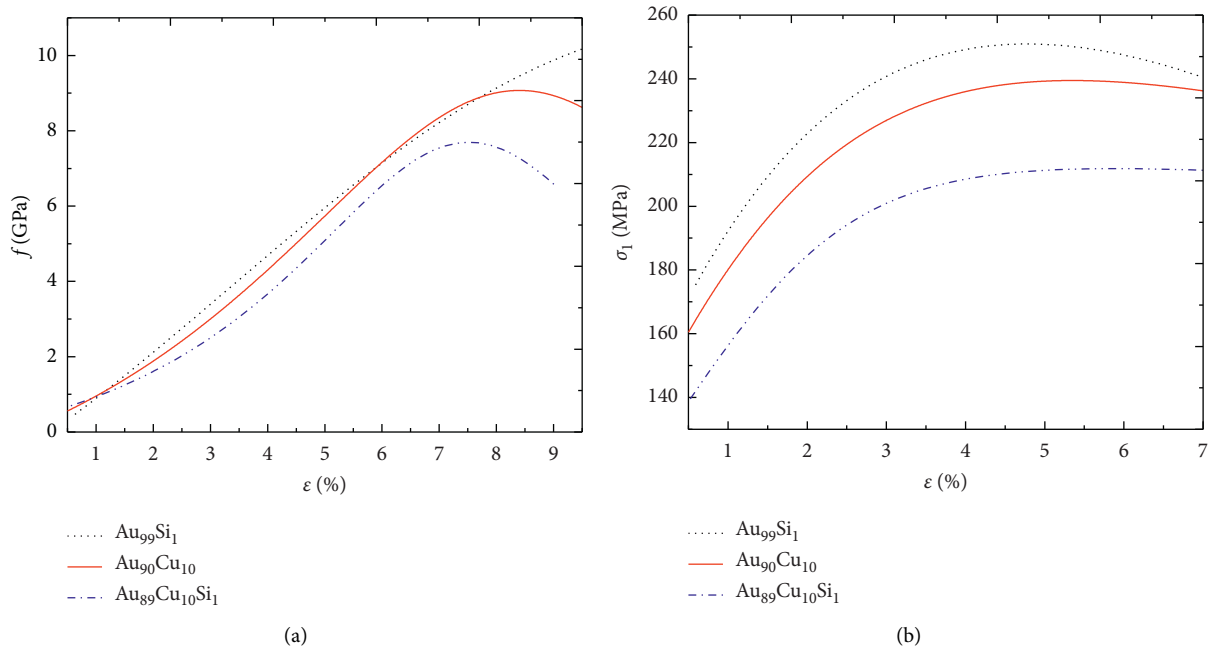

FIGURE 3: The density of deformation energy $f(\varepsilon)$ (a) and the real stress $\sigma_1(\varepsilon)$ (b) of $Au_{99}Si_1$, $Au_{90}Cu_{10}$, and $Au_{89}Cu_{10}Si_1$ at $T = 300$ K and $P = 0$ calculated by the SMM.

TABLE 4: Values of ε_F ($f(\varepsilon_F) = f_{max}$), σ_{1max}, ε_e, and σ_e for $Au_{99}Si_1$, $Au_{90}Cu_{10}$, and $Au_{89}Cu_{10}Si_1$ at $P = 0$ and $T = 300$ K calculated by the SMM.

Alloy	ε_F (%)	σ_{1max} (MPa)	ε_e (%)	σ_e (MPa)
$Au_{99}Si_1$	9.6	214.07	0.18	165.49
$Au_{90}Cu_{10}$	8.3	242.95	0.19	196.75
$Au_{89}Cu_{10}Si_1$	8.2	216.79	0.19	175.98

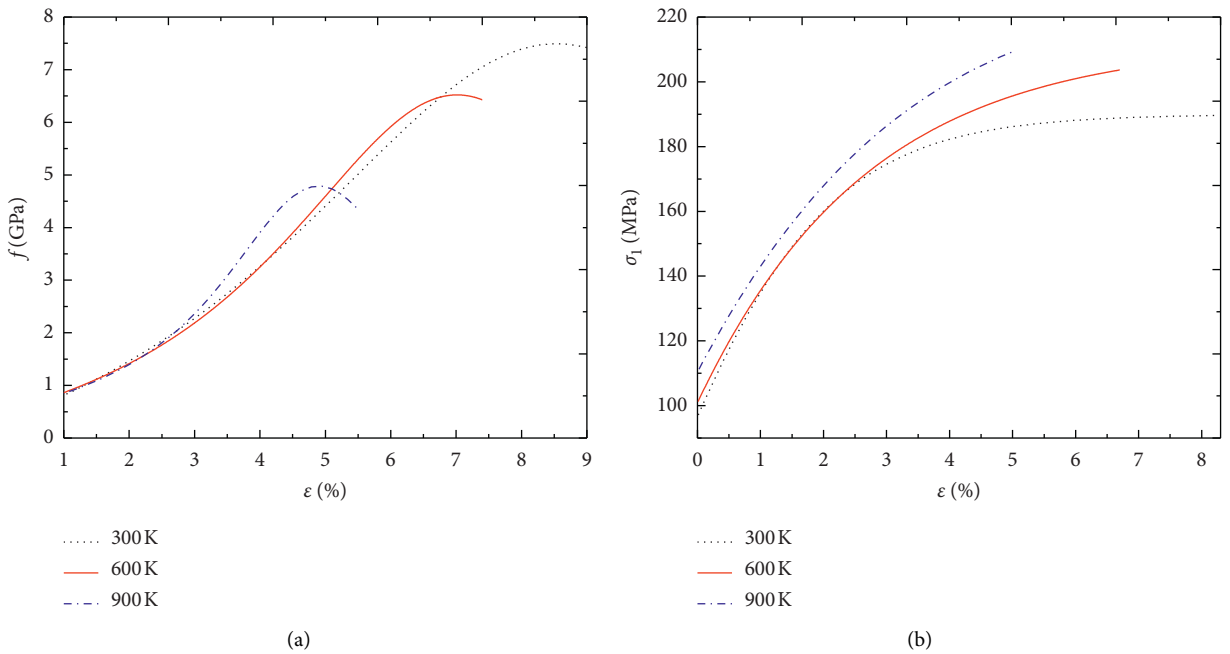

FIGURE 4: The density of deformation energy $f(\varepsilon)$ (a) and the real stress $\sigma_1(\varepsilon)$ (b) of $Au_{88}Cu_{10}Si_2$ at $P = 0$ and $T = 300$, 600, and 900 K calculated by the SMM.

Table 5: Values of ε_F ($f(\varepsilon_F) = f_{\max}$), $\sigma_{1\max}$, ε_e, and σ_e for $Au_{88}Cu_{10}Si_2$ at $P = 0$ and $T = 300$, 600, and 900 K calculated by the SMM.

T (K)	ε_F (%)	$\sigma_{1\max}$ (MPa)	ε_e (%)	σ_e (MPa)
300	8.2	194.52	0.18	157.36
600	6.7	208.29	0.24	179.85
900	5.0	210.27	0.32	193.19

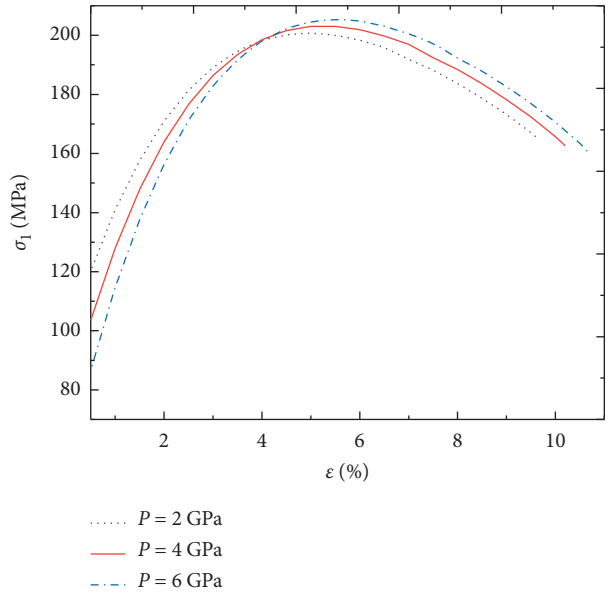

Figure 5: The real stress $\sigma_1(\varepsilon)$ of $Au_{87}Cu_{10}Si_3$ at $P = 2$, 4, and 6 GPa and $T = 300$ K calculated by the SMM.

Table 6: Values of ε_F ($f(\varepsilon_F) = f_{\max}$), $\sigma_{1\max}$, ε_e, and σ_e for $Au_{88}Cu_{10}Si_2$ at $P = 2$, 4, and 6 GPa and $T = 300$ K calculated by the SMM.

P (GPa)	ε_F (%)	$\sigma_{1\max}$ (MPa)	ε_e (%)	σ_e (MPa)
2	8.9	175.86	0.14	149.50
4	9.7	170.64	0.10	137.75
6	10.2	152.06	0.08	123.20

4. Conclusion

In our paper, we derive the analytic expressions of characteristic quantities for the nonlinear deformation such as the density of deformation energy, the maximum real stress, and the limit of elastic deformation depending on temperature, pressure, and concentration of components together with the strain-stress of substitutional alloy AB with interstitial atom C and FCC structure under pressure. We apply theoretical results to alloy AuCuSi. The maximum real stress $\sigma_{1\max}$ and the elastic limit σ_e calculated by the SMM are in good agreement with MD results [16] and experiments [13, 14]. For AuCuSi at the same temperature, concentration of substitutional atoms, and concentration of interstitial atoms, when the pressure increases, the maximum real stress increases and the elastic limit decreases. When the pressure increases from 2 to 4 GPa, the maximum real stress increases by 3% and the elastic limit decreases by 7.86%. When the pressure increases from 4 to 6 GPa, the maximum real stress increases by 11% and the elastic limit decreases by 10.56%. Our calculated results for alloy AuCuSi are compared with ones for alloys AuCu, AuSi, and metal Au. If we use more coordination spheres and we have exact experimental data for the stress $\sigma_{0.2}$ of alloy AuCuSi at different temperatures, pressures, and concentrations of components, we will obtain better calculations.

Data Availability

The data that support the findings of this study are available from the corresponding author upon reasonable request.

Conflicts of Interest

The authors declare that they have no conflicts of interest.

References

[1] A. Smirnov, *Theory Of Interstitial Alloys*, Nauka, Moscow, Russia, in Russian, 1979.

[2] P. A. Korzhavyi, I. A. Abrikosov, B. Johansson, A. V. Ruban, and H. L. Skriver, "First-principles calculations of the vacancy formation energy in transition and noble metals," *Physical Review B*, vol. 59, no. 18, p. 11693, 1999.

[3] T. T. Lau, C. J. Först, X. Lin, J. G. Gale, S. Yip, and K. J. Van Vliet, *Physical Review Letter*, vol. 98, Article ID 215501, 2007.

[4] M. Li, "Defect-induced topological order-to-disorder transition in two-dimensional binary substitutional solid solutions," *Physical Review B*, vol. 62, Article ID 13979, 2000.
[5] N. Q. Hoc and N. D. Hien, "42nd vietnam national Conference on theoretical physics (NCTP-42)," *IOP Conference Series: Journal of Physics: Conference Series*, vol. 1034, Article ID 012005, 2018.
[6] N. Q. Hoc, B. D. Tinh, and N. D. Hien, "Elastic moduli and elastic constants of alloy aucusi with fcc structure under pressure," *High Temperature Materials and Processes*, vol. 38, pp. 264–272, 2018.
[7] B. D. Tinh, N. Q. Hoc, D. Q. Vinh, T. D. Cuong, and N. D. Hien, *Advances in Materials Science and Engineering*, vol. 2018, p. 8, Article ID 5251741, 2018.
[8] N. Q. Hoc, T. D. Cuong, and N. D. Hien, "Proceedings of the ACCMS-theme meeting on "Multiscale modelling of materials for sustainable development"" *VNU Journal of Sciences: Mathematics-Physics*, vol. 35, no. 1, pp. 1–12, 2019.
[9] N. Q. Hoc, B. D. Tinh, and N. D. Hien, *Romanian Journal of Physics*, vol. 65, no. 5-6, p. 608, 2020.
[10] N. Q. Hoc, N. T. Hoa, T. D. Cuong, and D. Q. Thang, "On the melting of interstitial alloys FeH, FeSi and FeC with a body-centered cubic structure under pressure Proceedings of the ACCMS-theme meeting on "multiscale modelling of materials for sustainable development"" *Vietnam Journal of Science, Technology and Engineering*, vol. 61, no. 2, pp. 17–22, 2019.
[11] R. D. Nyilas, M. Kobas, and R. Spolenak, "Synchrotron X-ray microdiffraction reveals rotational plastic deformation mechanisms in polycrystalline thin films," *Acta Materialia*, vol. 57, no. 13, pp. 3738–3753, 2009.
[12] I. Chasiotis, C. Bateson, K. Timpano, A. S. McCarty, N. S. Barker, and J. R. Stanec, "Strain rate effects on the mechanical behavior of nanocrystalline Au films," *Thin Solid Films*, vol. 515, no. 6, pp. 3183–3189, 2007.
[13] https://structx.com/Material_Properties_003a.html.
[14] https://www.azom.com/properties.aspx?ArticleID=600.
[15] M. J. Mehl and D. A. Papaconstantopoulos, "Applications of a tight-binding total-energy method for transition and noble metals: elastic constants, vacancies, and surfaces of monatomic metals," *Physical Review B*, vol. 54, no. 7, p. 4519, 1996.
[16] M. N. Esfahani and M. Jabbari, "Molecular dynamics simulations of deformation mechanisms in the mechanical response of nanoporous gold," *Materials*, vol. 13, no. 9, p. 2071, 2020.
[17] N. T. Dung, N. C. Cuong, and D. Q. Van, *Journal of Multiscale Modelling*, vol. 11, no. 2, Article ID 2030001, 2020.
[18] N. T. Dung and N. T. Phuong, "Molecular dynamics study on factors influencing the structure, phase transition and crystallization process of NiCu6912 nanoparticle," *Materials Chemistry and Physics*, vol. 250, Article ID 123075, 2020.
[19] T. Q. Tuan and N. T. Dung, "Effect of heating rate, impurity concentration of Cu, atomic number, temperatures, time annealing temperature on the structure, crystallization temperature and crystallization process of Ni1−xCux bulk; $x = 0.1$, 0.3, 0.5, 0.7," *International Journal of Modern Physics B*, vol. 32, no. 26, p. 1830009, 2018.
[20] C. L. Van, D. Q. Van, and N. T. Dung, "Ab initio calculations on the structural and electronic properties of AgAu alloy," *ACS Omega*, vol. 5, no. 48, pp. 31391–31397, 2020.
[21] N. Tang and V. V. Hung, "Investigation of the thermodynamic properties of anharmonic crystals by the momentum method, I. General results for face-centered cubic crystals," *Physica Status Solidi (B)*, vol. 149, p. 511, 1989.
[22] N. Tang and V. Van Hung, "Investigation of the thermodynamic properties of anharmonic crystals by the momentum method. II. Comparison of calculations with experiments for inert gas crystals," *Physica Status Solidi (B)*, vol. 161, no. 1, p. 165, 1990.
[23] N. Tang and V. Van Hung, "Investigation of the thermodynamic properties of anharmonic crystals by the momentum method. III. Thermodynamic properties of the crystals at various pressures," *Physica Status Solidi (B)*, vol. 162, no. 2, p. 371, 1990.
[24] N. Tang and V. Van Hung, "Investigation of the thermodynamic properties of anharmonic crystals by momentum method. IV. The limiting of absolute stability and the melting temperature of crystals," *Physica Status Solidi (B)*, vol. 162, no. 2, p. 379, 1990.
[25] M. N. Magomedov, "On calculating the Debye temperature and the Gruneisen parameter," *Zhurnal Fizicheskoi Khimii*, vol. 61, no. 4, pp. 1003–1009, 1987, in Russian.
[26] R. J. Good and C. J. Hope, "New combining rule for intermolecular distances in intermolecular potential functions," *The Journal of Chemical Physics*, vol. 53, no. 2, pp. 540–543, 1970.
[27] M. N. Magomedov, "The calculation of the parameters of the Mie-Lennard-Jones potential," *High Temperature*, vol. 44, no. 4, pp. 513–529, 2006.
[28] E. Goens, *Physikal. Z.*vol. 37, p. 321, 1936.
[29] F. Birch, "Finite elastic strain of cubic crystals," *Physical Review*, vol. 71, no. 11, p. 809, 1947.
[30] B. Bayram, O. Akar, and T. Akin, "Plasma-activated direct bonding of diamond-on-insulator wafers to thermal oxide grown silicon wafers," *Diamond and Related Materials*, vol. 19, no. 11, pp. 1431–1435, 2010.
[31] Z. Y. Zhong, H. Saka, T. H. Kim, E. A. Holm, Y. K. Han, and X. S. Xie, "Effect of pressure on melting temperature of silicon and germanium," *Materials Science Forum*, vol. 475–479, pp. 1893–1896, 2005.
[32] D. Errandonea, *Journal of Applied Physics*, vol. 108, Article ID 033517, 2010.
[33] D. Errandonea, "High-pressure melting curves of the transition metals Cu, Ni, Pd and Pt," *Physical Review B*, vol. 87, Article ID 054108, 2013.
[34] L. V. Tikhonov and G. I. Kononenko, *Mechanical Properties of Metals and Alloys*, Kiev–Nauka Dumka, Ukraine, 1986.